CHEMISTRY OF MATERIALS

pubs.acs.org/cm

Article

Control over the Geometric Shapes and Mechanical Properties of Uniform Platelets via Tunable Two-Dimensional Living Self-Assembly

Liyang Fu, Yanxue Che, Yanjun Gong,* Hongwei Ji, Yifan Zhang, Ling Zang,* Jincai Zhao, and Yanke Che*

Cite This: *Chem. Mater.* 2023, 35, 1310−1317

Read Online

ACCESS | Metrics & More | Article Recommendations | Supporting Information

ABSTRACT: It remains unexplored how the living self-assembly of small molecules can gain control over the geometric shapes and mechanical properties of the two-dimensional (2D) platelets fabricated therefrom. Herein, we report a tunable 2D living self-assembly method to control the geometric shape variety and mechanical properties of the resulting uniform 2D platelets. This new approach of using *n*-alkyl alcohols to connect a donor−acceptor (D−A) molecule into a 2D network via hydrogen bonding has a threefold effect on the formed 2D platelets. First, the intralayer molecular packing involving continuous hydrogen bonds between a D−A fluorophore and alcohols remains unaltered, thereby yielding the same optical properties and thermal stability to various 2D platelets. Second, the kinetic growth differentiation of the D−A fluorophore and alcohol in two dimensions depends on the interaction competition of alcohol with the D−A fluorophore against hexane (a poor solvent), engendering the alcohol-dependent 2D shape variety. Third, the interlayer interactions along the thickness of the platelet can be effectively modulated by the alcohol tails with different lengths that stretch out of each bilayer, thereby varying the mechanical properties of the 2D platelets, for which Young's moduli and hardnesses decrease significantly with the increasing tail length of the alcohols.

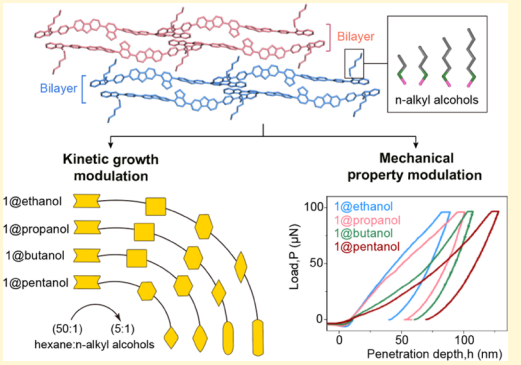

INTRODUCTION

Living seeded self-assembly, an emerging powerful strategy for fabricating soft materials, has unparalleled advantages in fabricating uniform complex architectures with controlled sizes.[1−10] The crystallization-driven living self-assembly of block copolymers into various complex one-dimensional (1D) and two-dimensional (2D) structures pioneered by Manners and co-workers represents a considerably successful example.[1−3,11,12] However, for small molecules, only 1D structures with controlled lengths can be grown using living seeded self-assembly methods.[4−9,13−23] The seeded growth of small molecules into uniform 2D structures with tailorable shapes and sizes, rather than in an irregular format,[10,24] remains a formidable challenge for the aforementioned living self-assembly. The requirements for precise control of the growth kinetics in two dimensions are likely beyond the approaches for 1D living self-assembly of small molecules.

We recently developed a novel living self-assembly strategy for fabricating uniform 2D platelets with various shapes and controlled sizes, where a two-component nucleus was formed using 1-hexanol and a donor−acceptor (D−A) molecule via continuous alternative hydrogen bonds.[25] Despite this encouraging development, the application potential of the two-component-based living self-assembly method remains unknown. For example, there is a question of whether the unique continuous alternative hydrogen bond connection between two components can be engineered to exert kinetic effects on nucleus formation, which in turn reshapes 2D structures. There is another question of whether the mechanical properties (e.g., the elasticity and hardness) can be effectively modulated without altering the geometric shape or thermodynamic properties of 2D structures using tunable 2D living self-assembly. Extensive experimental exploration and mechanistic investigations are required to address these critical questions.

In this work, we report a tunable 2D living self-assembly method, i.e., using various *n*-alkyl alcohols to connect a D−A molecule **1** via hydrogen bonding in two dimensions, to produce uniform 2D platelets with controlled shapes and mechanical properties (Figure 1). We first demonstrate that, despite using different alcohols, considerably similar continuous alternative hydrogen bonds were formed between **1** and

Received: November 7, 2022
Revised: January 5, 2023
Published: January 16, 2023

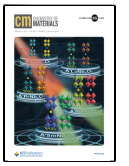

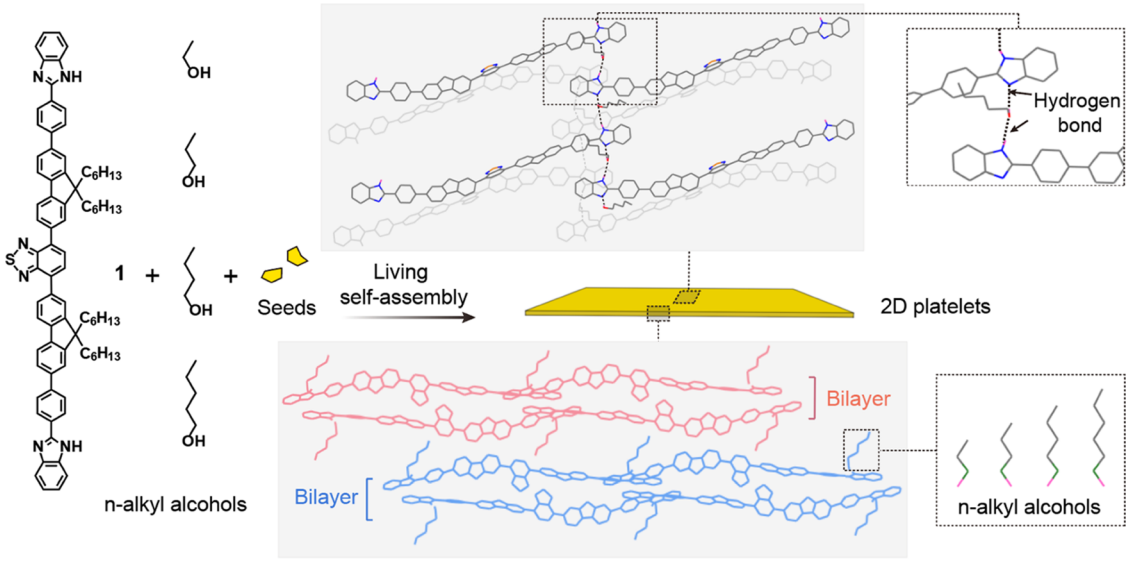

Figure 1. Schematic of 2D living self-assembly of four *n*-alkyl alcohols (i.e., ethanol, propanol, butanol, and pentanol) and a D−A fluorophore **1**, presenting the intralayer continuous alternative intermolecular hydrogen bonds and the alkyl tail of alcohol stretching out on each bilayer.

alcohols within the resulting 2D structures (Figure 1), engendering their similar optical properties and thermal stability. Second, the kinetics of the hydrogen bond formation from various alcohols and **1** varied in two dimensions because of the interaction competition among alcohols with **1** against hexane (a poor solvent); the kinetic growth differentiation therefore creates the alcohol-dependent 2D shape variety in the same solvent environments. Third, the interlayer interactions along the thickness of 2D platelets could be altered by alcohol tails with different lengths stretched out on each bilayer, enabling the effective modulation of the mechanical properties of 2D platelets. The nanoindentation measurements demonstrate that Young's moduli and hardnesses of 2D platelets decreased from 6.0 GPa and 289.2 MPa for **1**@ethanol platelets to 4.3 GPa and 232 MPa for **1**@pentanol platelets. Thus, we found that the tunable 2D living self-assembly method opens up a new avenue for developing small molecule-based 2D platelets with a wide range of geometric shapes and optimized mechanical properties.

EXPERIMENTAL SECTION

Synthesis of Fluorophore 1. The synthesis of fluorophore **1** was performed by following a previously reported method.[25]

Fluorophore **1**: ^{1}H NMR (400 MHz, THF-d8): δ: 11.83 (s, 2H), 8.32, 8.30 (d, J = 8.0 Hz, 4H), 8.25 (s, 2H), 8.15, 8.13 (d, J = 8.0 Hz, 2H), 8.06 (s, 2H), 8.00−7.92 (m, 8H), 7.87 (s, 2H), 7.82, 7.80 (d, J = 8.0 Hz, 2H), 7.73, 7.72, 7.70 (m, J = 4.0 Hz, 2H), 7.50, 7.49, 7.47 (m, J = 4.0 Hz, 2H), 7.21, 7.20, 7.19 (m, J = 4.0 Hz, 4H), 2.27−2.22 (q, J = 2.0 Hz, 8H), 1.20−1.17 (m, 24H), 0.91−0.89 (m, 8H), 0.83, 0.82, 0.81 (m, J = 4.0 Hz, 12H) (Figure S1). ^{13}C NMR (175 MHz, $CDCl_3$/CD_3OD = 3:1, ppm): δ: 159.8, 152.1, 151.2, 151.1, 143.9, 140.7, 140.5, 138.7, 137.0, 135.2, 128.4, 128.3, 127.6, 127.1, 126.8, 126.0, 124.1, 123.3, 121.2, 120.2, 119.5, 114.4, 55.2, 40.1, 31.2, 29.4, 23.7, 22.3, 13.5. (Figure S2). MALDI-MS: (m/z) =1185.7 (Figure S3).

Fabrication of 2D Platelets from 1. 2D platelets from **1** and ethanol (**1**@ethanol platelets), which were used to prepare seeds, were first self-assembled by injecting a 0.1 mL solution of **1** (0.5 mg/mL) in an ethanol/chloroform mixture (v/v, 3:1) into 2 mL hexane in a 4 mL vial, followed by aging for 24 h at room temperature. Notably, chloroform herein was added to increase the solubility of **1** in alcohols; the same procedure was used throughout this work, though not specifically mentioned. The 2D platelets thus prepared were sonicated at −20 °C for 8 h to produce **1**@ethanol seeds, which were generally of irregular shapes. The areas of the resulting seeds range from 0.6 to 7.2 μm^2.

Living seeded self-assembly of 2D platelets with controlled shapes was performed upon the addition of a certain volume of the feed solution of **1** into the seed solution in the same solvent mixtures in a vial. For example, 2D **1**@ethanol platelets were self-assembled by adding a freshly prepared feed solution of **1** to the seed solution (0.025 mg/mL, 0.01 mL) in hexane/ethanol mixtures with varying volume ratios from 50:1 to 5:1 (v/v) and subsequently aging for 24 h at room temperature. The feed solution of **1** with varying hexane/ethanol volume ratios was prepared by adding different volumes of hexane to the solution of **1** (0.5 mg/mL, 0.1 mL) in an ethanol/chloroform mixture (v/v, 3:1). The same procedure was applied to the seeded self-assembly of **1** and other alcohols, including methanol and various bulky alcohols.

Property Characterizations and Theoretical Calculations. *Property Characterizations.* Fluorescence-mode optical microscopic images were obtained from an inverted fluorescence microscope (Olympus X71). Single crystal X-ray diffraction (SXRD) measurements were carried out on a Rigaku XtaLAB PRO 007HF diffractometer equipped with graphite monochromatized Cu Kα (λ = 1.54184 Å) radiation in the ω scan mode. The structure was solved by intrinsic phasing (SHELXT) and refined by full-matrix least squares on F^2(SHELXL-2014). Ultraviolet−visible (UV−vis) spectra of 2D platelets with different shapes were obtained using a UV−visible−NIR microscope (CRAIC Technologies, Inc.). The samples were drop-cast onto a glass substrate and dried in air. Time-dependent absorption spectra of **1** in different hexane/alcohol mixtures for monitoring the kinetics of the seeded self-assembly were obtained using a Hitachi U-3900 spectrometer. Differential scanning calorimetry (DSC) measurements were conducted on a TA instrument DSC-Q2000 under nitrogen in the temperature range from 50 to 300 °C with a heating and subsequent cooling rate of 10 °C min^{-1}. Photoluminescence quantum yields (PLQYs) of 2D platelets were determined using a Hamamatsu Absolute PL quantum yield spectrometer C11247 coupled with an integrating sphere. Atomic force microscopy (AFM) nanoindentation measurements were performed using an HYSITRON TI980 instrument equipped with a Berkovich probe, which had a 350 mm stainless steel cantilever, at the end of which a triangular pyramidal diamond indenter tip was mounted.

Theoretical Calculations. Elastic moduli (E^*) of 2D platelets were calculated based on the force−displacement curves measured by AFM nanoindentation experiments. Assuming an elastic contact between

https://doi.org/10.1021/acs.chemmater.2c03339
Chem. Mater. 2023, 35, 1310−1317

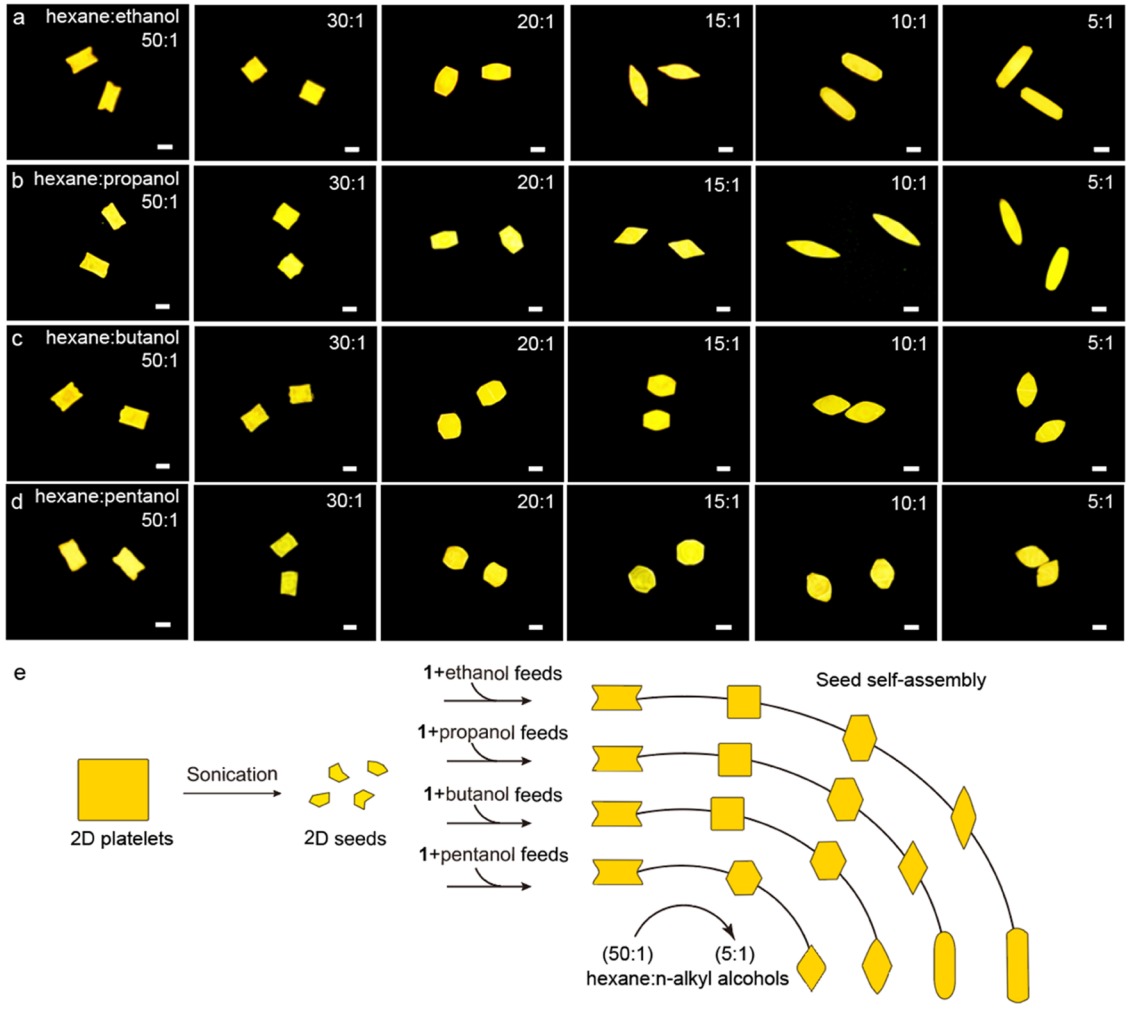

Figure 2. (a–d) Fluorescence-mode optical images of 2D platelets formed via living seeded self-assembly of **1** in different hexane/*n*-alkyl alcohol mixtures with volume ratios ranging from 50:1 to 5:1 (left to right); scale bars = 10 μm. (e) A schematic of the seeded growth of 2D platelets in which the shape variety is dependent on the alcohol used.

the cone and the flat specimen, the force and indenter displacement could be obtained using the following Sneddon's equations[26]

$$P = \frac{2}{\pi}E^{*}\tan\alpha h^{2} \tag{1}$$

where P is the maximum force, E^{*} is the reduced elastic modulus, α is the indenter cone half-angle, and h is the displacement of the specimen free surface beneath the indenter. eq. 1 can be further converted into eq. 2

$$\frac{dP}{dh} = 2\left[\frac{2}{\pi}E^{*}\tan\alpha\right]h \tag{2}$$

where dP/dh is defined as the contact stiffness.

The displacement of the indenter (h) and the radius of the circle of contact (a) can be further expressed as the following equation

$$h = \frac{\pi}{2}a\cot\alpha \tag{3}$$

and since $A = \pi a^{2} = \pi(\tan\alpha h)^{2}$, the following equation can be obtained.

$$E^{*} = \frac{1}{2}\frac{dP}{dh}\frac{\sqrt{\pi}}{\sqrt{A}} \tag{4}$$

Hardness (H), which is defined as the resistance to local plastic/permanent deformation, can be calculated by dividing the applied load(P) by the contact area (A).[27] In a nanoindentation measurement, hardness (H) can be calculated following eq. 5, where the contact area A can be obtained from the indentation depth (h) at the maximum load (P)

$$H = \frac{P_{max}}{A_{c}} = \frac{P_{max}}{\pi(\tan\alpha h_{t})^{2}} \tag{5}$$

RESULTS AND DISCUSSION

Tunable 2D Living Self-Assembly Using Various Alcohols. Various alcohols, including primary (i.e., ethanol, propanol, butanol, and pentanol), secondary (i.e., 3-pentanol), and tertiary alcohols (i.e., *t*-butanol and *t*-amyl alcohol), were selected to modify the living seeded self-assembly of **1**. Irregular seeds with surface areas ranging from 0.6 to 7.2 μm^2 were prepared by sonicating the prefabricated rectangular 2D platelets at −20 °C for 8 h. Subsequently, a feed solution of **1** (0.5 mg/mL, 0.1 mL) in hexane/alcohol mixtures with varying hexane/alcohol volume ratios (50:1 to 5:1) was added to the seed solution (0.025 mg/mL, 0.01 mL) with the same solvent mixture to proceed the living seeded self-assembly. The morphology of the resulting assemblies was monitored and characterized via fluorescence optical microscopy. Figures 2 and S4–S7 show the geometric shapes of 2D platelets formed in the hexane/alcohol mixtures with varying volume ratios.

https://doi.org/10.1021/acs.chemmater.2c03339
Chem. Mater. 2023, 35, 1310−1317

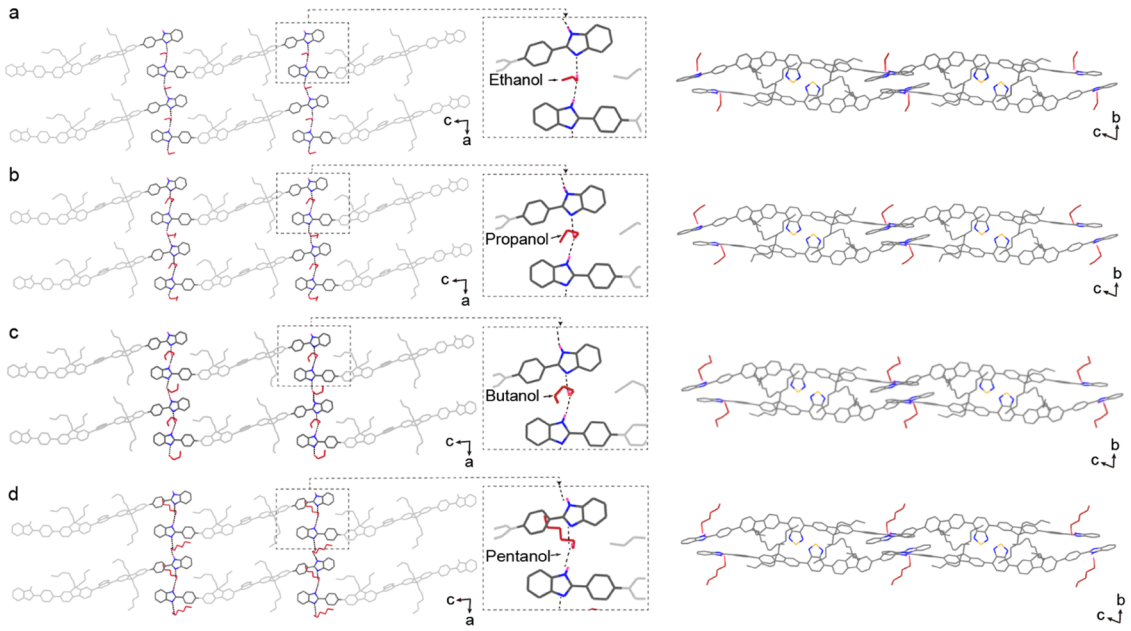

Figure 3. Molecular packing of the four crystals: (a) **1**@ethanol, (b) **1**@propanol, (c) **1**@butanol, and (d) **1**@pentanol.

Apparently, the resulting 2D shape variety depended on the selected alcohol; the shape variety gradually decreased with an increase in the tail length of *n*-alkyl alcohols (Figure 2e). For example, five geometric shapes of 2D structures, including an incomplete rectangle, a square, a hexagon, a diamond, and a rounded rectangle, were formed when ethanol was involved in the aforementioned seeded self-assembly (Figure 2a). Conversely, when pentanol was used under the same self-assembly conditions, only three shapes of 2D platelets were formed: an incomplete rectangle, a hexagon, and a diamond (Figure 2d). We also examined the effect of alcohol mixtures on the geometries of the resulting 2D platelets. Figure S8 shows that fine-tuning the aspect ratio of the 2D shapes rather than creating a new shape was achieved using mixed alcohols. Atomic force microscopy (AFM) analysis of all the aforementioned 2D platelets showed that their thicknesses fall in a relatively narrow range from 150 to 300 nm, regardless of their different shapes (Figure S9). These results indicate that the applied alcohols have no prominent influence on the thicknesses of formed 2D platelets. Notably, methanol or bulky secondary and tertiary alcohols could not induce the formation of uniform 2D platelets but formed other irregular structures (Figures S10−S13), suggesting that alcohols with an appropriate size are necessary to form continuous alternative hydrogen bonds for 2D platelets. Furthermore, methanol may be too small and bulky alcohols may be too large to fit in for yielding continuous alternative hydrogen bonds. Optical characterizations show that all the 2D platelets with different shapes exhibited almost identical absorption and emission spectra and emission efficiency (Figures S14 and S15 and Table S1), despite the different alcohols involved to achieve the 2D connection. This indicates that these platelets shared the same molecular packing of fluorophore **1**, which in turn determines the optical properties. This conclusion was further confirmed by powder X-ray diffraction (XRD) measurements (Figure S16), which indicated that the 2D platelets of different shapes had the same lamellar structure where an interlayer distance of 1.6 nm was observed along the thickness direction.

Molecular Packing within 2D Platelets. Single-crystal X-ray diffraction analysis of bulky crystals grown using **1** and four *n*-alkyl alcohols (i.e., **1**@ethanol, **1**@propanol, **1**@butanol, and **1**@pentanol) was performed to obtain detailed information regarding the molecular packing of various 2D platelets. The detailed growth of bulky crystals suitable for single-crystal analysis is provided in the Supporting Information. As shown in Figure 3 and Table S2, fluorophore **1** and all four alcohols acted as both donors and acceptors to form continuous alternative hydrogen bonds to enable the intralayer crystal growth in two dimensions. The intermolecular distance of **1** within the four crystals is the same: 4.4 Å along the *a*-axis and 5.1 Å along the *c*-axis. Given the large intermolecular spacing of **1** along the *b*-axis (>9.0 Å), the intralayer molecular interactions of **1** within the *a*-*c* plane should make a dominant contribution to the optical properties of the 2D platelets.

In this regard, the identical intralayer molecular packing explains well the aforementioned identical optical properties of the 2D platelets fabricated with the four *n*-alkyl alcohols. Compared to the loose interlayer packing along the *b* axis (>9.0 Å), the dense intralayer molecular connection is also expected to determine the thermal stability of the 2D platelets, which thereby was expected to be similar among the four platelets. Indeed, as characterized by differential scanning calorimetry, all four platelets assembled with different alcohols exhibited a similar phase transition with an endothermic peak at around 275 °C (Figures S17 and S18). This transition should be related to the alcohol release and the subsequent intermolecular reorganization. The related details have been investigated in our laboratory and will be published in the near future. Such a high transition temperature is remarkable for molecular assemblies or related soft materials. This observation also suggests that the molecular connection via 2D continuous hydrogen bonds may be a promising approach for fabricating 2D structures with high thermal stability.

Of note, along the *b* axis of the 2D crystals (Figure 3), the alcohol tails with different lengths are stretched out on the back-to-back layers (termed as bilayer). Therefore, the interactions between bilayers are expected to be modulated

https://doi.org/10.1021/acs.chemmater.2c03339
Chem. Mater. 2023, 35, 1310−1317

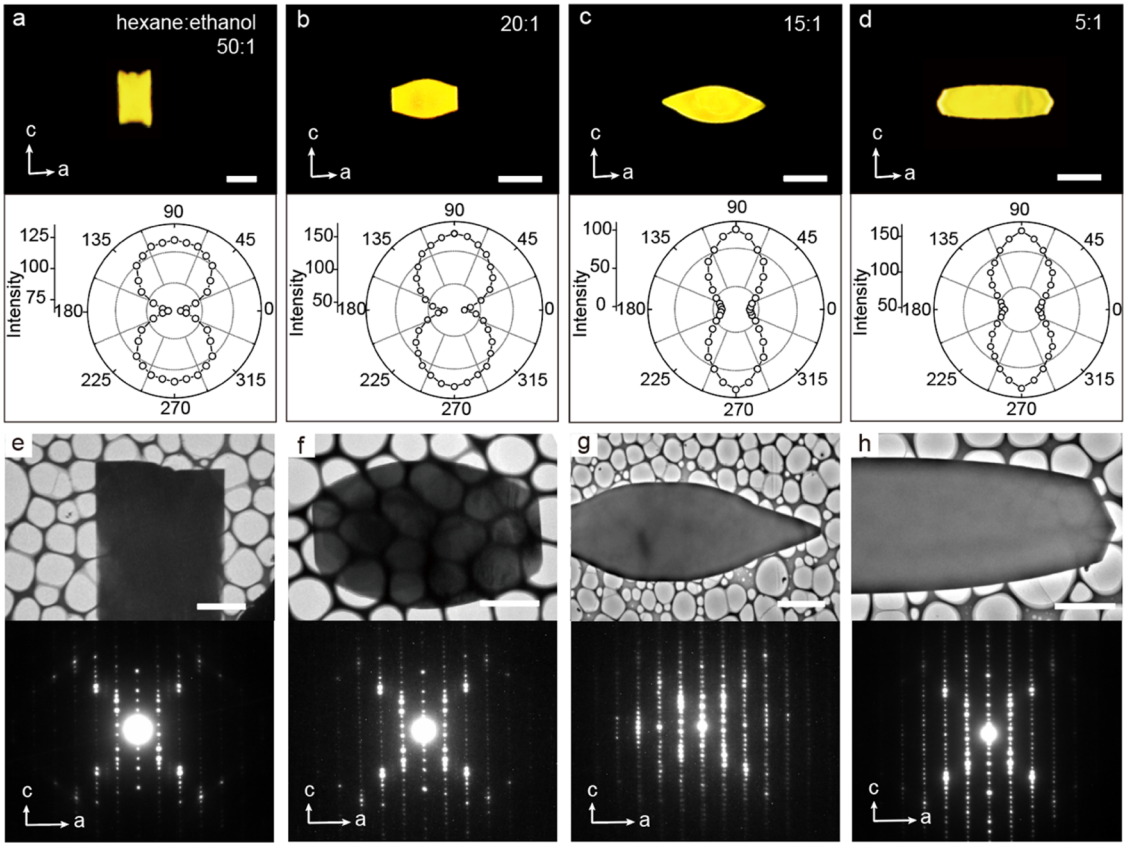

Figure 4. (a–d) Fluorescence-mode optical images of **1**@ethanol 2D platelets prepared in hexane/ethanol mixtures with different volume ratios of (a) 50:1, (b) 20:1, (c) 15:1, and (d) 5:1 and their corresponding polarized emissions along the long axis; scale bars = 10 μm. (e–h) TEM images and selective area electron diffraction patterns of the 2D platelets assembled under the same conditions as (a–d), respectively; scale bars = 5 μm.

by the alcohol tails with different lengths, which in turn can alter the mechanical properties of the resulting 2D platelets (see discussion below).

Kinetic Growth Differentiation in Two Dimensions for Various Geometric Shapes of 2D Platelets. Given the same intralayer molecular packing in the aforementioned 2D platelets, the formation of distinct geometric shapes should arise from kinetic growth differentiation in two dimensions rather than thermodynamic control. To support this hypothesis, we measured the polarized emission of **1**@ethanol 2D platelets with different shapes fabricated under different volume ratios of hexane/alcohol, which was used to locate the molecular orientation of **1** in the 2D platelets. As shown in Figure 4a, the molecular orientation of **1**, as revealed by the polarized emission, was consistent with the length of the incomplete, rectangular-like 2D platelet formed in a hexane/ethanol (v/v, 50:1) mixture. This observation indicates that the growth rate of **1** along the *c*-axis, i.e., parallel to the direction of the molecular long axis (Figure 3), was faster than that along the *a* axis in this solvent environment. With the volume ratio of hexane/ethanol decreasing, the growth along the *a* axis gets more kinetically competitive than that along the *c*-axis, and thus the length vs width of the resulting 2D structure began to reverse (Figure 4a–d). Specifically, when the volume ratio of hexane/ethanol decreased below 30:1, the growth along the *a* axis became faster than that along the *c*-axis, resulting in the formation of 2D platelets in a predominantly elongated shape along the *a* axis. This indicates that the growth rate of **1** along the *a*-axis relative to the *c*-axis is kinetically favorable in the presence of more alcohols. Further evidence for the distinct molecular orientation of **1** within the 2D platelets with different shapes was obtained through selected area electron diffraction analysis. Figure 4e–h illustrates electron diffraction patterns for the corresponding 2D platelets, which are consistent with the polarized emission results (Figure 4a–d). These observations allowed us to conclude that the volume ratio of hexane and alcohol could effectively modulate the kinetic growth differentiation of **1** and alcohol in two dimensions, thereby generating 2D platelets with different shapes.

Interestingly, alcohols with different tail lengths yielded different growth rates for 2D platelets in the solvent mixture with the same hexane/alcohol ratio (Figure S19); the longer the alcohol tail, the slower the growth of 2D platelets. This is because the increasing hydrophobic interactions between the long-tail alcohol and hexane can attenuate the kinetic involvement of alcohol in forming continuous hydrogen bonds with **1**. The increasing interactions with the solvent would diminish the kinetic growth differentiation in two dimensions, thereby leading to a narrowed shape variety of the 2D platelets (Figure 2). conversely, the short-tail alcohol, e.g., ethanol, had relatively weak interactions with hexane, thus providing more kinetic freedom to modulate 2D growth for creating more geometric shapes than the long-tail alcohol.

Modulation of Mechanical Properties of 2D Platelets by Alcohols with Different Tail Lengths. In addition to the kinetical growth differentiation of **1** and alcohols in two dimensions toward different 2D shapes, various alcohols with varying alkyl tail lengths were expected to influence the mechanical properties along the thickness (i.e., the *b* axis) of

https://doi.org/10.1021/acs.chemmater.2c03339
Chem. Mater. 2023, 35, 1310–1317

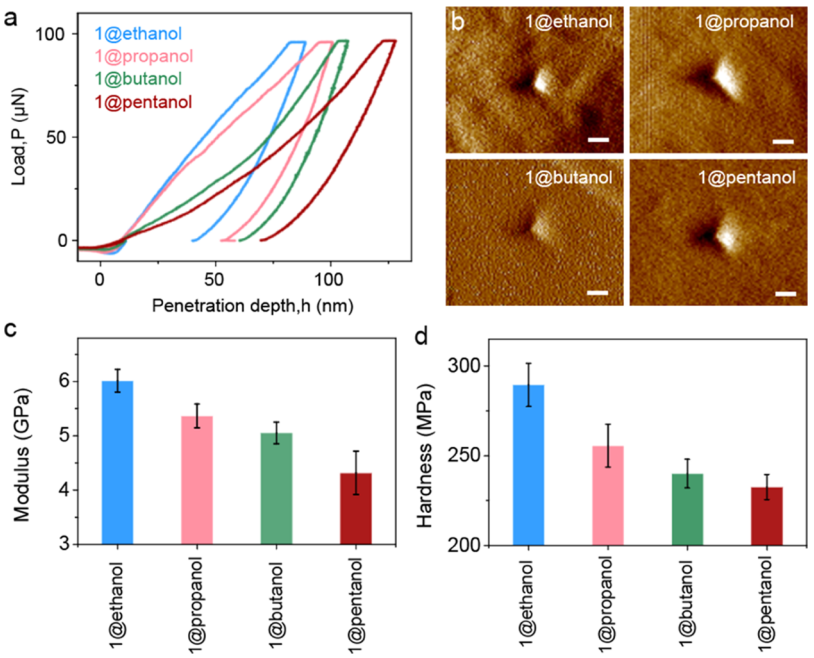

Figure 5. (a) Load−displacement curves of four **1**@alcohol 2D platelets (i.e., **1**@ethanol, **1**@propanol, **1**@butanol, and **1**@pentanol) formed in a hexane/alcohol mixture (v/v, 5:1). (b) Surface micrograph of the four 2D platelets after the nanoindentation test. (c, d) Comparison of calculated Young's moduli (c) and hardnesses (d) between the four 2D platelets.

2D platelets. To verify this, we performed nanoindentation tests on the typical diamond-like 2D platelets formed using four different alcohols.

We used a triangular pyramidal diamond indenter tip to press the 2D platelets on a silica substrate and release them to obtain the load− and unload−displacement curves as shown in Figure 5. Based on the obtained curves (Figure 5a,b), Young's moduli and hardnesses were calculated for the four platelets along the *b*-axis (Figure 5c,d). The results indicate that these 2D platelets are typical soft materials.[28−33] Intriguingly, both Young's moduli and hardnesses of 2D structures remarkably decreased with increasing alcohol tail length, indicating that longer alcohols could effectively reduce the interlayer interactions and thereby decrease Young's moduli and hardnesses of the 2D platelets. These results demonstrate that the mechanical properties of the 2D platelets could be modulated by simply using alcohols with different tail lengths, without altering the geometric shape and optical and thermodynamic properties of the platelets.

CONCLUSIONS

We have achieved control over the geometric shape variety and mechanical properties of 2D platelets through tunable 2D living self-assembly, for which various *n*-alkyl alcohols are employed to connect fluorophore **1** in two dimensions via hydrogen bonding. The single-crystal analysis demonstrates that various alcohols and fluorophore **1** adopt the same continuous alternative hydrogen bonding to achieve intralayer molecular packing, while the alkyl tails of alcohols extend out on each bilayer to interact with each other. Despite the very similar optical and thermodynamical properties resulting from the same intralayer molecular packing, the kinetic growth differentiation of **1** and alcohols in two dimensions, which arises from the interaction competition between alcohol−**1** and alcohol−hexane, generates the alcohol-dependent 2D shape variety. Furthermore, the different interlayer interactions between the alcohol tails with different lengths extended on each bilayer effectively modulate the mechanical properties of 2D platelets, such as Young's modulus and hardness. The work reported herein opens a new avenue to develop small molecule-based 2D structures requiring extended geometry shapes, controlled sizes, and optimizable mechanical properties. These novel functional 2D materials may find wide applications in fluorescence imaging, sensing, and nonlinear optical materials.

ASSOCIATED CONTENT

Supporting Information

The Supporting Information is available free of charge at https://pubs.acs.org/doi/10.1021/acs.chemmater.2c03339.

^{1}H NMR, ^{13}C NMR, and MALDI-MS spectra of fluorophore **1**; additional property characterizations of 2D platelets and other assemblies; ^{1}H NMR, characterizations of fluorophore **1**PDF)

AUTHOR INFORMATION

Corresponding Authors

Yanjun Gong − *Key Laboratory of Photochemistry, CAS Research/Education Center for Excellence in Molecular Sciences, Institute of Chemistry, Chinese Academy of Sciences, Beijing 100190, China; University of Chinese Academy of Sciences, Beijing 100049, China*; Email: yjgong0612@iccas.ac.cn

Ling Zang − *Nano Institute of Utah, and Department of Materials Science and Engineering, University of Utah, Salt Lake City, Utah 84112, United States*; orcid.org/0000-0002-4299-0992; Email: lzang@eng.utah.edu

Yanke Che − *Key Laboratory of Photochemistry, CAS Research/Education Center for Excellence in Molecular Sciences, Institute of Chemistry, Chinese Academy of Sciences, Beijing 100190, China; University of Chinese Academy of*

Sciences, Beijing 100049, China; orcid.org/0000-0002-9671-3704; Email: ykche@iccas.ac.cn

Authors

Liyang Fu − *Key Laboratory of Photochemistry, CAS Research/Education Center for Excellence in Molecular Sciences, Institute of Chemistry, Chinese Academy of Sciences, Beijing 100190, China; University of Chinese Academy of Sciences, Beijing 100049, China*

Yanxue Che − *HT-NOVA Co., Ltd., Beijing 101312, China*

Hongwei Ji − *Key Laboratory of Photochemistry, CAS Research/Education Center for Excellence in Molecular Sciences, Institute of Chemistry, Chinese Academy of Sciences, Beijing 100190, China; University of Chinese Academy of Sciences, Beijing 100049, China*

Yifan Zhang − *Key Laboratory of Photochemistry, CAS Research/Education Center for Excellence in Molecular Sciences, Institute of Chemistry, Chinese Academy of Sciences, Beijing 100190, China; University of Chinese Academy of Sciences, Beijing 100049, China;* orcid.org/0000-0003-1298-5436

Jincai Zhao − *Key Laboratory of Photochemistry, CAS Research/Education Center for Excellence in Molecular Sciences, Institute of Chemistry, Chinese Academy of Sciences, Beijing 100190, China; University of Chinese Academy of Sciences, Beijing 100049, China;* orcid.org/0000-0003-1449-4235

Complete contact information is available at: https://pubs.acs.org/10.1021/acs.chemmater.2c03339

Notes

The authors declare no competing financial interest.

■ ACKNOWLEDGMENTS

This work was funded by NSFC (No. 21925604), the National Key Research and Development Program of China (No. 2019YFA0210401), and the Strategic Priority Research Program of the Chinese Academy of Sciences (Grant No. XDB36000000).

■ REFERENCES

(1) Jin, X. H.; Price, M. B.; Finnegan, J. R.; Boott, C. E.; Richter, J. M.; Rao, A.; Menke, S. M.; Friend, R. H.; Whittell, G. R.; Manners, I. Long-range exciton transport in conjugated polymer nanofibers prepared by seeded growth. *Science* **2018**, *360*, 897−900.

(2) Qiu, H.; Gao, Y.; Boott, C. E.; Gould, O. E. C.; Harniman, R. L.; Miles, M. J.; Webb, S. E. D.; Winnik, M. A.; Manners, I. Uniform patchy and hollow rectangular platelet micelles from crystallizable polymer blends. *Science* **2016**, *352*, 697−701.

(3) He, X.; Hsiao, M. S.; Boott, C. E.; Harniman, R. L.; Nazemi, A.; Li, X.; Winnik, M. A.; Manners, I. Two-dimensional assemblies from crystallizable homopolymers with charged termini. *Nat. Mater.* **2017**, *16*, 481−488.

(4) Choi, H.; Ogi, S.; Ando, N.; Yamaguchi, S. Dual Trapping of a Metastable Planarized Triarylborane pi-System Based on Folding and Lewis Acid-Base Complexation for Seeded Polymerization. *J. Am. Chem. Soc.* **2021**, *143*, 2953−2961.

(5) Ogi, S.; Sugiyasu, K.; Manna, S.; Samitsu, S.; Takeuchi, M. Living supramolecular polymerization realized through a biomimetic approach. *Nat. Chem.* **2014**, *6*, 188−195.

(6) Ogi, S.; Matsumoto, K.; Yamaguchi, S. Seeded Polymerization through the Interplay of Folding and Aggregation of an Amino-Acid-based Diamide. *Angew. Chem., Int. Ed.* **2018**, *57*, 2339−2343.

(7) Kang, J.; Miyajima, D.; Mori, T.; Inoue, Y.; Itoh, Y.; Aida, T. A rational strategy for the realization of chain-growth supramolecular polymerization. *Science* **2015**, *347*, 646−651.

(8) Chen, Z.; Suzuki, Y.; Imayoshi, A.; Ji, X.; Rao, K. V.; Omata, Y.; Miyajima, D.; Sato, E.; Nihonyanagi, A.; Aida, T. Solvent-free autocatalytic supramolecular polymerization. *Nat. Mater.* **2022**, *21*, 253−261.

(9) Aliprandi, A.; Mauro, M.; De Cola, L. Controlling and imaging biomimetic self-assembly. *Nat. Chem.* **2016**, *8*, 10−15.

(10) Fukui, T.; Kawai, S.; Fujinuma, S.; Matsushita, Y.; Yasuda, T.; Sakurai, T.; Seki, S.; Takeuchi, M.; Sugiyasu, K. Control over differentiation of a metastable supramolecular assembly in one and two dimensions. *Nat. Chem.* **2017**, *9*, 493−499.

(11) Fukui, T.; Garcia-Hernandez, J. D.; MacFarlane, L. R.; Lei, S.; Whittell, G. R.; Manners, I. Seeded Self-Assembly of Charge-Terminated Poly(3-hexylthiophene) Amphiphiles Based on the Energy Landscape. *J. Am. Chem. Soc.* **2020**, *142*, 15038−15048.

(12) Zhang, Y.; Pearce, S.; Eloi, J. C.; Harniman, R. L.; Tian, J.; Cordoba, C.; Kang, Y.; Fukui, T.; Qiu, H.; Blackburn, A.; Richardson, R. M.; Manners, I. Dendritic Micelles with Controlled Branching and Sensor Applications. *J. Am. Chem. Soc.* **2021**, *143*, 5805−5814.

(13) Weyandt, E.; Leanza, L.; Capelli, R.; Pavan, G. M.; Vantomme, G.; Meijer, E. W. Controlling the length of porphyrin supramolecular polymers via coupled equilibria and dilution-induced supramolecular polymerization. *Nat. Commun.* **2022**, *13*, No. 248.

(14) Sarkar, A.; Sasmal, R.; Das, A.; Venugopal, A.; Agasti, S. S.; George, S. J. Tricomponent Supramolecular Multiblock Copolymers with Tunable Composition via Sequential Seeded Growth. *Angew. Chem., Int. Ed.* **2021**, *60*, 18209−18216.

(15) Liu, B.; Pappas, C. G.; Ottele, J.; Schaeffer, G.; Jurissek, C.; Pieters, P. F.; Altay, M.; Maric, I.; Stuart, M. C. A.; Otto, S. Spontaneous Emergence of Self-Replicating Molecules Containing Nucleobases and Amino Acids. *J. Am. Chem. Soc.* **2020**, *142*, 4184−4192.

(16) Wan, Q.; To, W.-P.; Chang, X.; Che, C.-M. Controlled Synthesis of PdII and PtII Supramolecular Copolymer with Sequential Multiblock and Amplified Phosphorescence. *Chem* **2020**, *6*, 945−967.

(17) Sarkar, A.; Behera, T.; Sasmal, R.; Capelli, R.; Empereur-Mot, C.; Mahato, J.; Agasti, S. S.; Pavan, G. M.; Chowdhury, A.; George, S. J. Cooperative Supramolecular Block Copolymerization for the Synthesis of Functional Axial Organic Heterostructures. *J. Am. Chem. Soc.* **2020**, *142*, 11528−11539.

(18) Rao, K. V.; Mabesoone, M. F. J.; Miyajima, D.; Nihonyanagi, A.; Meijer, E. W.; Aida, T. Distinct Pathways in ″Thermally Bisignate Supramolecular Polymerization″: Spectroscopic and Computational Studies. *J. Am. Chem. Soc.* **2020**, *142*, 598−605.

(19) Vantomme, G.; Ter Huurne, G. M.; Kulkarni, C.; Ten Eikelder, H. M. M.; Markvoort, A. J.; Palmans, A. R. A.; Meijer, E. W. Tuning the Length of Cooperative Supramolecular Polymers under Thermodynamic Control. *J. Am. Chem. Soc.* **2019**, *141*, 18278−18285.

(20) Greciano, E. E.; Matarranz, B.; Sanchez, L. Pathway Complexity Versus Hierarchical Self-Assembly in N-Annulated Perylenes: Structural Effects in Seeded Supramolecular Polymerization. *Angew. Chem., Int. Ed.* **2018**, *57*, 4697−4701.

(21) Haedler, A. T.; Meskers, S. C.; Zha, R. H.; Kivala, M.; Schmidt, H. W.; Meijer, E. W. Pathway Complexity in the Enantioselective Self-Assembly of Functional Carbonyl-Bridged Triarylamine Trisamides. *J. Am. Chem. Soc.* **2016**, *138*, 10539−10545.

(22) Ma, X.; Zhang, Y.; Zhang, Y.; Liu, Y.; Che, Y.; Zhao, J. Fabrication of Chiral-Selective Nanotubular Heterojunctions through Living Supramolecular Polymerization. *Angew. Chem., Int. Ed.* **2016**, *55*, 9539−9543.

(23) Ogi, S.; Stepanenko, V.; Sugiyasu, K.; Takeuchi, M.; Wurthner, F. Mechanism of self-assembly process and seeded supramolecular polymerization of perylene bisimide organogelator. *J. Am. Chem. Soc.* **2015**, *137*, 3300−3307.

(24) Sasaki, N.; Mabesoone, M. F. J.; Kikkawa, J.; Fukui, T.; Shioya, N.; Shimoaka, T.; Hasegawa, T.; Takagi, H.; Haruki, R.; Shimizu, N.; Adachi, S. I.; Meijer, E. W.; Takeuchi, M.; Sugiyasu, K. Supra-

molecular double-stranded Archimedean spirals and concentric toroids. *Nat. Commun.* **2020**, *11*, No. 3578.
(25) Gong, Y.; Cheng, C.; Ji, H.; Che, Y.; Zang, L.; Zhao, J.; Zhang, Y. Unprecedented Small Molecule-Based Uniform Two-Dimensional Platelets with Tailorable Shapes and Sizes. *J. Am. Chem. Soc.* **2022**, *144*, 15403−15410.
(26) Sneddon, I. N. The Relation Between Load and Penetration in the Axisymmetric Boussinesq Problem for a Punch of Arbitrary Profile. *Int.. J. Eng. Sci.* **1965**, *3*, 47−57.
(27) Tabor, D.*The Hardness of Metals*; Clarendon Press: Oxford, 1951; Chapter 2.
(28) Rus, D.; Tolley, M. T. Design, fabrication and control of soft robots. *Nature* **2015**, *521*, 467−475.
(29) Saha, S.; Desiraju, G. R. Acid···Amide Supramolecular Synthon in Cocrystals: From Spectroscopic Detection to Property Engineering. *J. Am. Chem. Soc.* **2018**, *140*, 6361−6373.
(30) Saha, S.; Mishra, M. K.; Reddy, C. M.; Desiraju, G. R. From Molecules to Interactions to Crystal Engineering: Mechanical Properties of Organic Solids. *Acc. Chem. Res.* **2018**, *51*, 2957−2967.
(31) Hayashi, S.; Koizumi, T. Elastic Organic Crystals of a Fluorescent pi-Conjugated Molecule. *Angew. Chem., Int. Ed.* **2016**, *55*, 2701−2704.
(32) Mishra, M. K.; Desiraju, G. R.; Ramamurty, U.; Bond, A. D. Studying microstructure in molecular crystals with nanoindentation: intergrowth polymorphism in felodipine. *Angew. Chem., Int. Ed.* **2014**, *53*, 13102−13105.
(33) Varughese, S.; Kiran, M. S.; Ramamurty, U.; Desiraju, G. R. Nanoindentation in crystal engineering: quantifying mechanical properties of molecular crystals. *Angew. Chem., Int. Ed.* **2013**, *52*, 2701−2712.

https://doi.org/10.1021/acs.chemmater.2c03339
Chem. Mater. 2023, 35, 1310−1317